• Photo-electric absorption is maximized in the ultra-violet and soft X-ray band. It has to be corrected for when performing X-ray spectroscopy in compact objects such as AGNs and neutron stars. The cross section for the PE effect above the threshold frequency ν_c scales roughly as $(\nu/\nu_c)^{-7/2}$.

$*$ The severity of the source spectral attenuation below around 5 keV is used to measure the integrated **column density** $n_e d$ along the line of sight to the source at distance d.

• Since the direction that an ejected electron emerges depends on the photon polarization (i.e. the orientation of its electric field vector), the photo-electric effect can be used as a tool for **X-ray polarimetry**.

Plot: Photo-electron Ejection Dependence on Light Polarization

1.2 Compton Scattering

A second watershed development in quantum theory was the identification by Compton in 1922 of the coupling between wavelength changes and the scattering angle θ in the collision between a photon and an electron. **C & O, Sec. 5.2**

$*$ the analytic relationship Compton identified is a direct consequence of light quantization as photons: $E_\gamma = hc/\lambda$.

Plot: Compton scattering

• If $E_\gamma = hc/\lambda = h\nu = p_\gamma c$ collides with an electron at rest, then conservation of (relativistic) energy and momentum gives

$$\boxed{\Delta\lambda \;\equiv\; \lambda_f - \lambda_i \;=\; \frac{h}{m_e c}\,(1-\cos\theta) \quad .} \tag{4}$$

• This change in wavelength is a purely quantum phenomenon, known as the **Compton effect**. Its discovery provided a major impetus for the development of quantum theory.

Polarization in the Photoelectric Effect

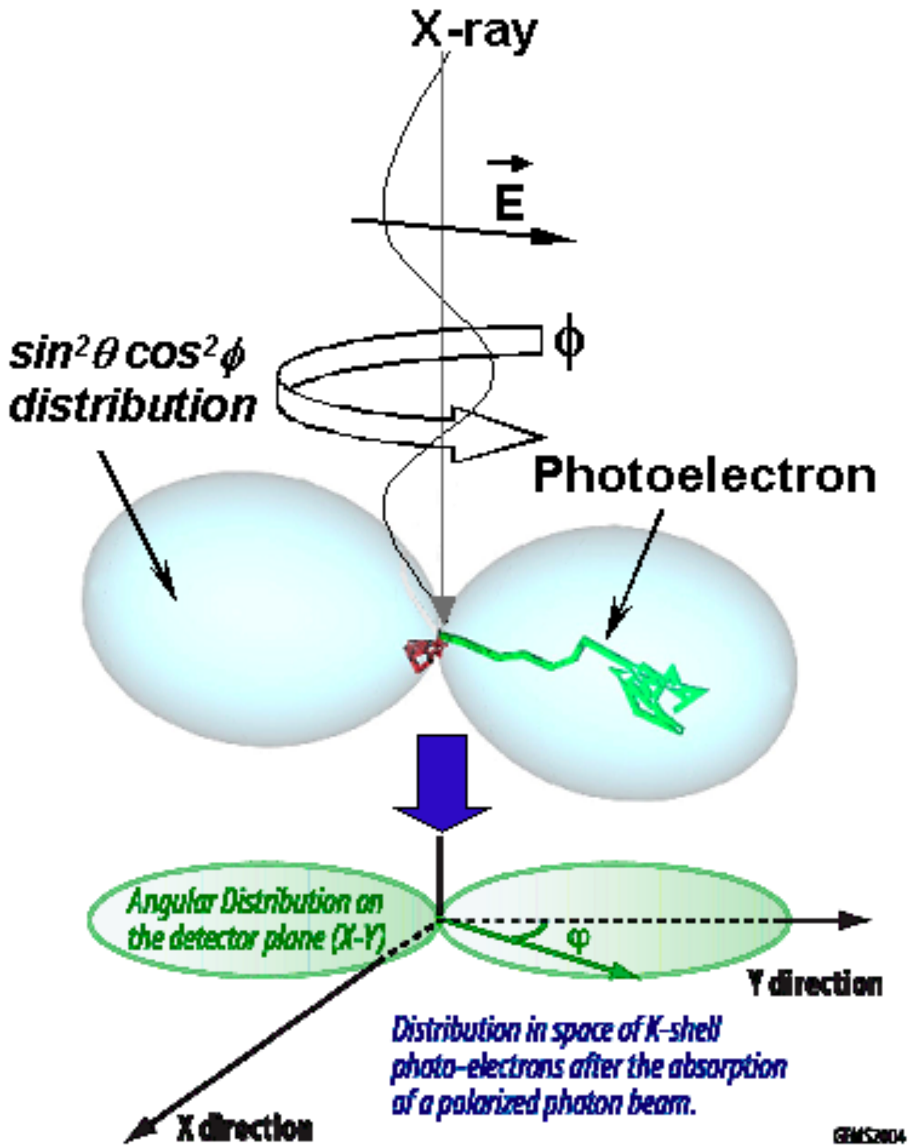

Electron-photon Compton Scattering

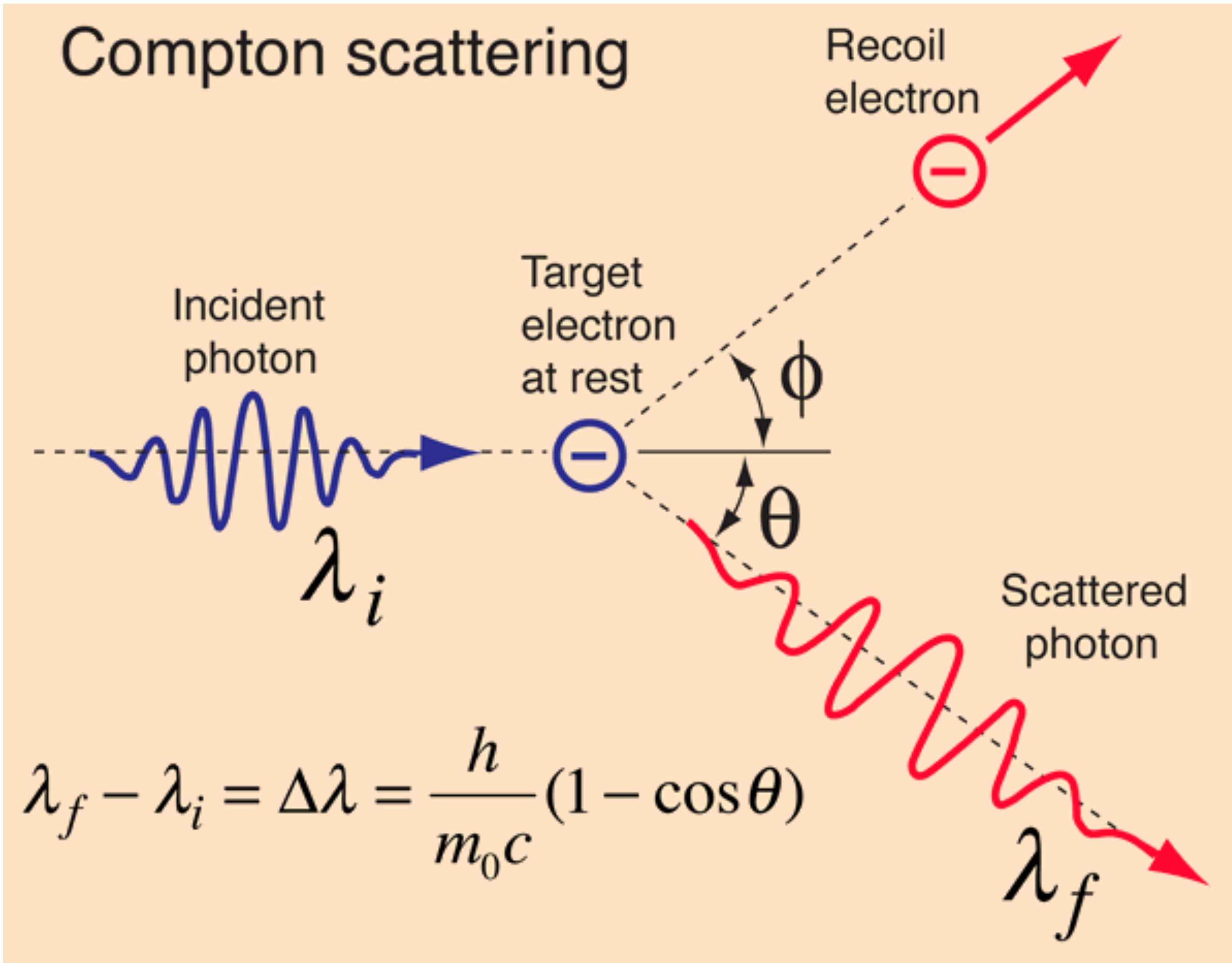

• Here, $h/(m_e c) = 2.426 \times 10^{-10}$ cm is known as the **Compton wavelength** of the electron; it represents the quantum spatial scale of the electron.

$*$ if we send $h \to 0$, so that quantum effects disappear, classical **Thomson scattering** still arises. This is realized in the long wavelength limit.

• The essentials of the Thomson process can be described using **Larmor formalism** for the radiation of accelerating charges. The power P per unit solid angle (averaged over all photon polarizations) is given by

$$\frac{dP}{d\Omega} \; = \; \frac{q^2}{8\pi c^3} \left(\dot{\mathbf{v}} \cdot \dot{\mathbf{v}} \right) \Bigl\{ 1 + \cos^2\theta \Bigr\} \quad \Rightarrow \quad P \; = \; \frac{2}{3} \frac{q^2 |\dot{\mathbf{v}}|^2}{c^3} \quad . \tag{5}$$

Here θ is the scattering angle of the photon. This differential power must be divided by the **Poynting flux** $S = \{|\mathbf{E}|^2 + |\mathbf{B}|^2\} c/(8\pi) \equiv |\mathbf{E}|^2 c/(4\pi)$ (light energy passing through unit area per unit time) to yield the **differential cross section** for scattering:

$$\frac{d\sigma}{d\Omega} \; = \; \frac{1}{S} \frac{dP}{d\Omega} \; = \; \frac{4\pi}{|\mathbf{E}|^2 c} \frac{dP}{d\Omega} \quad . \tag{6}$$

The mean electric field of the wave scales the electron acceleration through the Lorentz force, so that $m\, |\dot{\mathbf{v}}| = q |\mathbf{E}|$. One can then arrive at the **Thomson scattering cross section**. For unpolarized scattering, per unit solid angle, one has (for $q \to -e$)

$$\frac{d\sigma_{\rm T}}{d\Omega} \; = \; \frac{r_0^2}{2} \Bigl\{ 1 + \cos^2\theta \Bigr\} \quad , \quad r_0 \; = \; \frac{e^2}{m_e c^2} \; = \; 2.82 \times 10^{-13} \text{cm} \quad . \tag{7}$$

Here r_0 is the **classical electron radius**, and gives a measure of the "size" of the point charge in <u>classical</u> electromagnetic theory. Integrating over θ,

$$\sigma_{\rm T} \; = \; \frac{8\pi}{3} \, \alpha_{\rm f}^2 \left(\frac{\hbar}{m_e c} \right)^2 \; = \; \frac{8\pi}{3} \, r_0^2 \quad . \tag{8}$$

Here $\alpha_{\rm f} = e^2/\hbar c \approx 1/137.08$ is the **fine structure constant**, the fundamental coupling for interactions in **quantum electrodynamics** (QED).

• For $\lambda_i \lesssim h/(m_e c)$, extreme changes in the wavelength occur. This corresponds to photon energies $E_\gamma = hc/\lambda \sim m_e c^2$, and electron recoil becomes significant in the so-called **Klein-Nishina limit**.

1.3 Cyclotron and Synchrotron Radiation

• Cyclotron motion in a uniform magnetic field is described by the Lorentz force, which distills to space and time contributions for four-momentum $p^\mu \equiv (E,\, \mathbf{p}) = (\gamma mc^2,\, \gamma m\mathbf{v})$

$$\frac{d}{dt}\left(\gamma m\mathbf{v}\right) \;=\; \frac{q}{c}\mathbf{v}\times\mathbf{B} \quad , \quad \frac{d}{dt}\left(\gamma mc^2\right) \;=\; q\,\mathbf{v}_\perp\cdot\mathbf{B} \;=\; 0 \quad . \tag{9}$$

No work is done on the charge, so γ remains constant in time, neglecting radiation reaction. The equation of motion can then be separated to isolate the pieces for components of velocity parallel ($\mathbf{v}_\parallel \propto \mathbf{B}$) and perpendicular ($\mathbf{v}_\perp$) to the field:

$$\frac{d\mathbf{v}_\parallel}{dt} \;=\; 0 \quad , \quad \frac{d\mathbf{v}_\perp}{dt} \;=\; \frac{q}{\gamma mc}\,\mathbf{v}_\perp\times\mathbf{B} \quad . \tag{10}$$

The first of these is most easily deduced by writing $\mathbf{v} = \mathbf{v}_\parallel + \mathbf{v}_\perp$, and expanding the cross product, noting the trivial result $\mathbf{v}_\parallel\times\mathbf{B} = \mathbf{0}$.

• It follows that $\mathbf{v}_\parallel$ is constant, and therefore so also is $|\mathbf{v}_\perp|$, and the motion is helical. The frequency of the orbit or gyration is

$$\omega_{\rm B} \;=\; \frac{qB}{\gamma mc} \quad . \tag{11}$$

For a truly non-relativistic electron, <u>all</u> the radiation emerges at the cyclotron frequency. Yet, harmonics appear at the multiples $n\omega_{\rm B}$, for integers $n = 2, 3\ldots$, and these are suppressed in their power to the order of $(v/c)^{2n}$.

$\boxed{\textbf{Plot:}}$ Cyclotron Motion and Radiation

• For warm electrons, if $kT/m_ec^2 \sim v^2/c^2 \ll 1$, then the cyclotron fundamental is dominant, yet it is **Dopper broadened**. Eq. (11) would suggest that thermal motions might just redshift the fundamental at the $O(v^2/c^2)$ level, since $1/\gamma \approx 1 - v^2/(2c^2)$. Yet there is also blueshift+redshift in the $\mathbf{v}_\parallel$ component for an isotropic thermal gas, and this is of $O(v/c)$; this is what is dominant and defines the line broadening, with $\delta\nu/\nu \sim \sqrt{kT/m_ec^2}$.

Cyclotron and Synchrotron Radiation

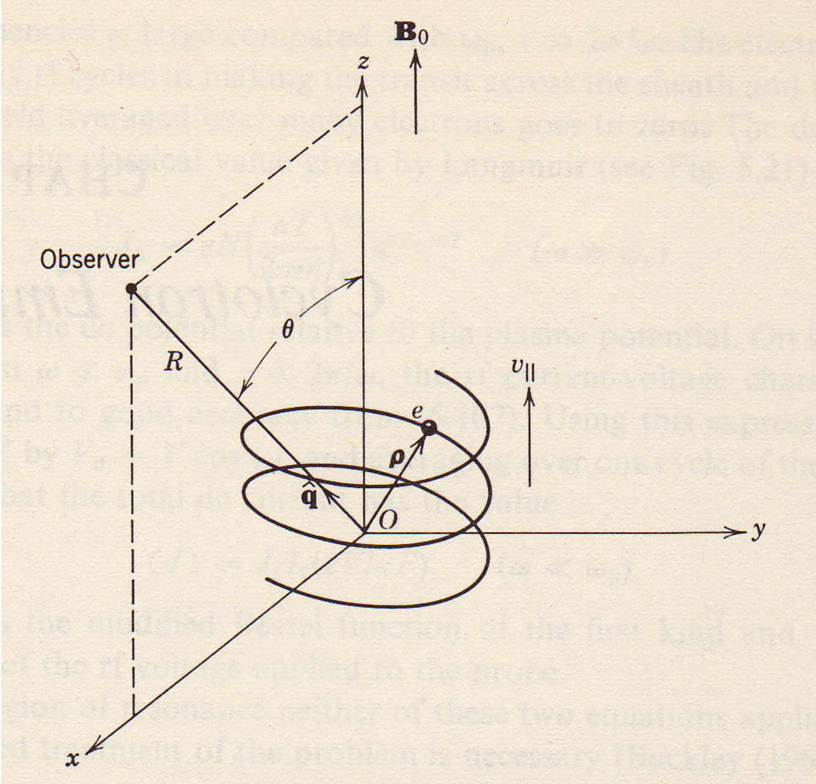

Fig. 6.1 Vector diagram for an electron in helical motion in a uniform magnetic field.

- From Bekefi (1966): "*Radiation Processes in Plasmas*"

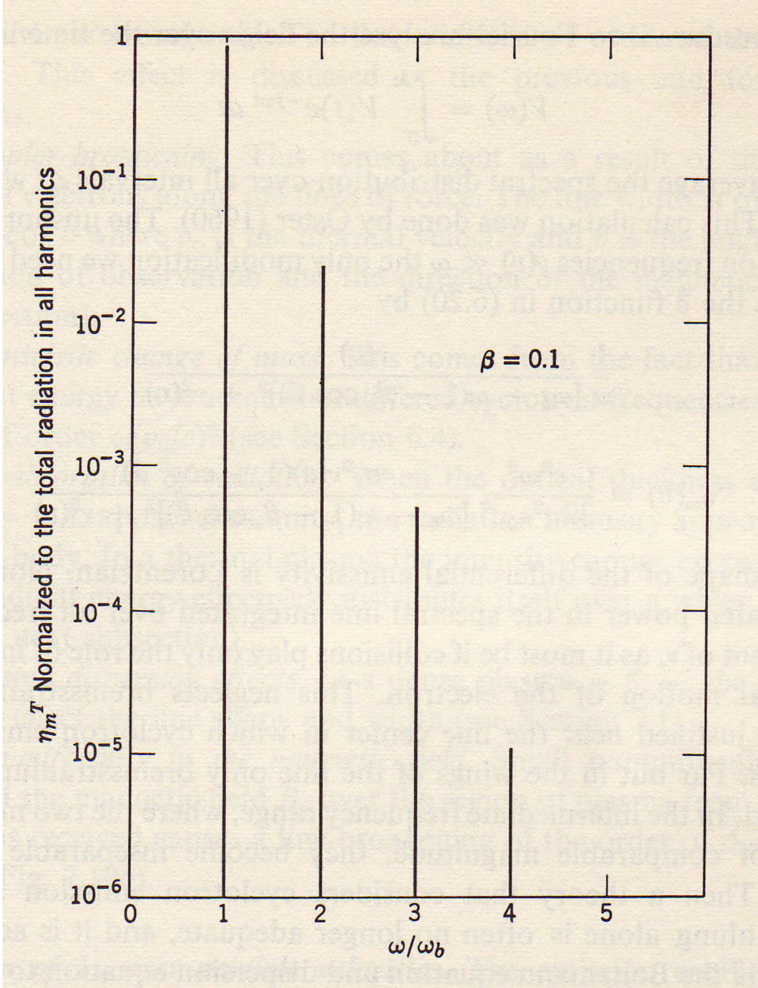

Fig. 6.2 Sketch of the spectrum of cyclotron radiation by a nearly nonrelativistic electron ($\beta_{\|} = 0$).

Cyclotron radiation is elliptically polarized in general, but is circularly polarized when viewing perpendicular to the plane of gyration, i.e. along $\mathbf{B}$.

• Total radiated power for acceleration is given by the Larmor formula in Eq. (5), but adapted for this problem, i.e., using $|\dot{\mathbf{v}}| = |\dot{\mathbf{v}}_\perp| = qB/\gamma m$:

$$P \;\equiv\; \frac{dE}{dt} \;=\; \frac{2}{3}\frac{q^2}{c^3}\gamma^4\left(\dot{\mathbf{v}}\cdot\dot{\mathbf{v}}\right) \;=\; \frac{2}{3}\frac{q^4}{m^2c^3}\gamma^2 B^2 \quad . \tag{12}$$

The extra factor of γ^4 is needed to describe the Doppler boosting of the radiated power (luminosity). Where does it come from? There are three contributions:

- the light frequency (and energy E) is blueshifted by γ ,
- the emitting time interval is shrunk by $1/\gamma$,
- the radiation is collimated (**beamed**) into a solid angle $\propto 1/\gamma^2$.

Clearly, for large enough γ , the radiation must rapidly cool the electrons and modify the helical motion: this we call **radiation reaction**.

• When the electron's motion is ultra-relativistic, with $\gamma \gg 1$, many cyclotron harmonics contribute, and the Doppler broadening is so substantial that the harmonics overlap. The result is a continuum spectrum for the process of **synchrotron radiation**.

$\boxed{\textbf{Plot:}}$ Synchrotron Radiation

• Synchrotron radiation is the principle emission mechanism from optically thin, magnetized plasmas with non-thermal electrons present, likely accelerated by astrophysical shocks or magnetic reconnection. It is seen in radio waves, optical, X rays and gamma rays. Manifestations include solar coronal field loops, supernova remnants, and relativistic jets near black holes.

$*$ Often, these settings involve power-law distributions of electrons, and so the radiation evinces approximately a non-thermal power-law spectrum.

$*$ Synchrotron radiation is highly polarized in general, though tangling of plasma magnetic fields can depolarize it significantly.

Synchrotron Beaming and Radio Sources

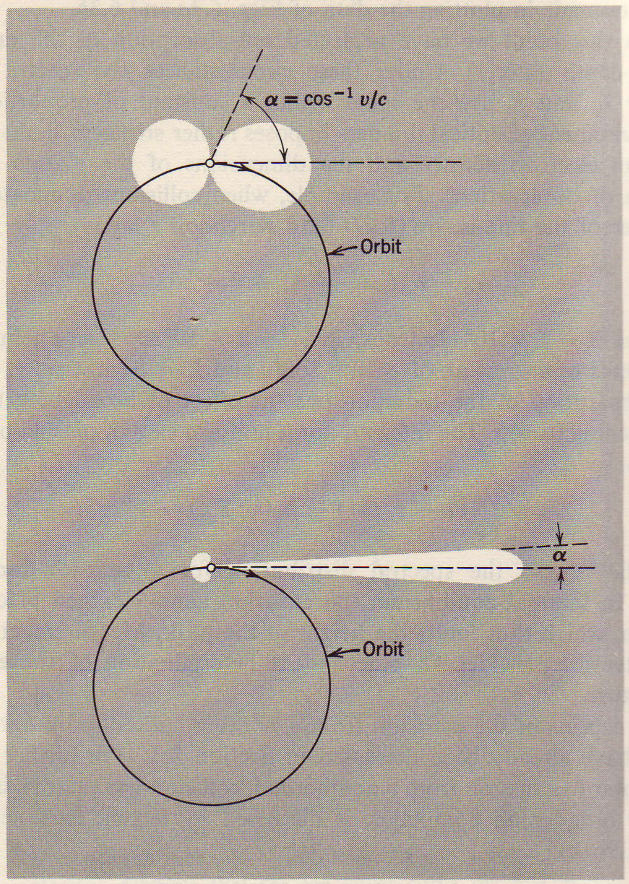

Fig. 6.5 A sketch of the polar diagram of the instantaneous radiation intensity of a nonrelativistic electron (above) and a highly relativistic electron (below). In the nonrelativistic case ($v/c \to 0$) the angular distribution is that of a dipole (3.11); the polar plot shown in the figure is a cross section of a doughnut-shaped object. In the highly relativistic case the polar plot shown is a cross section of a searchlight beam; the emission is predominantly along the instantaneous velocity vector of the charge. It is assumed that $\beta_\parallel = 0$. When $\beta_\parallel \neq 0$ the cone of radiation is again directed along the resultant velocity vector of the charge. [After Balwanz (1959).]

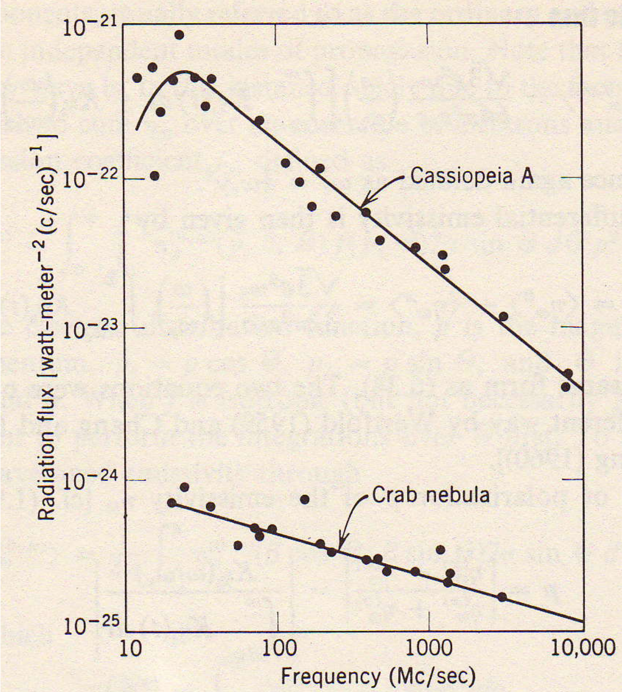

Fig. 6.8 Radiation flux from two astronomical objects. The experimental points represent observations of many workers in different observatories. [After Shklovsky (1960).]

- Synchrotron radiation is highly beamed and highly polarized (linear);
- High efficiency makes it prime emission mechanism in many sources (e.g. pulsars, Crab PWN, Cassiopeia A SNR)

1.4 Bremsstrahlung Radiation

• In ionized gases, *free-free* collisional interactions accelerate charges. Classically, these must radiate, and we call this **bremsstrahlung** emission. It can occur between free electrons, or in collisions of fast electrons with nuclei.

• The momentum deflection is small for large **impact parameters** b or electron speeds v, and for electron-ion collisions scales as

$$|\Delta \mathbf{p}| \approx \frac{2Ze^2}{bv} \tag{13}$$

The scattering angle is $\theta_{\rm sc} \approx |\Delta \mathbf{p}| / p$ and the probability of scattering is given by the differential cross section

$$\frac{d\sigma}{d\Omega} \approx \left(\frac{2Ze^2}{mv^2} \right)^2 \frac{1}{\theta_{\rm sc}^4} \quad . \tag{14}$$

This is the famous Coulomb scattering result discovered experimentally by Sir Ernest Rutherford, which led to the identification of compact, positively-charged nuclei in atoms. [Note the gravitational analog.]

Plot: Bremsstrahlung Collisional Geometry sketch

• Classically, bremsstrahlung is calculated as the radiative weighting of the Coulomb scattering process, and leads to flat spectra with temperatures tracing the gas temperature. The power dW per unit frequency interval $d\nu$ is

$$\frac{dW}{dV\, dt\, d\nu} \propto \frac{Z^2 n_e n_i}{\sqrt{kT}} \exp\left\{ -\frac{h\nu}{kT} \right\} \quad , \tag{15}$$

in unit volume dV and unit time dt.

• In astrophysics, bremsstrahlung is responsible for diffuse X-ray emission in the Galactic Ridge region, and in clusters of galaxies, with temperatures sometimes exceeding 10^7 K.

∗ Gravitational analog: collisions between massive bodies lead to gravitational radiation, much weaker than its electromagnetic counterpart.

Bremsstrahlung: Classical and Quantum

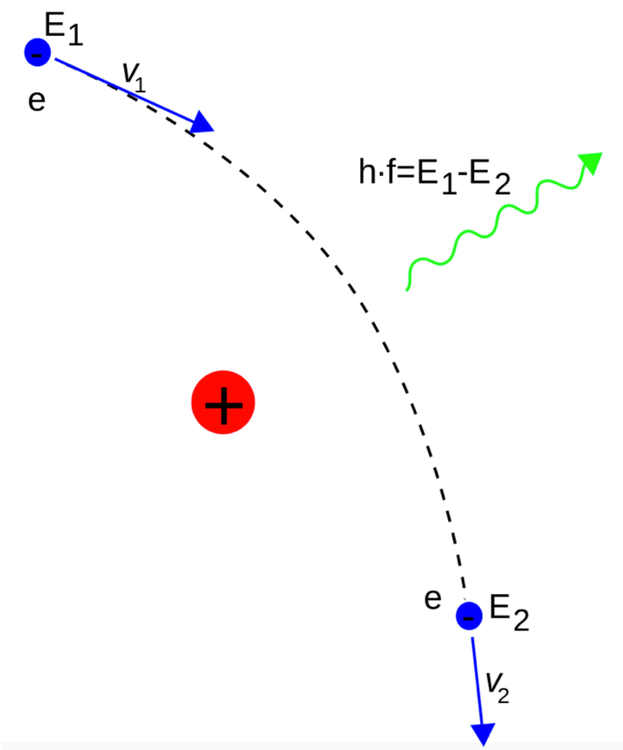

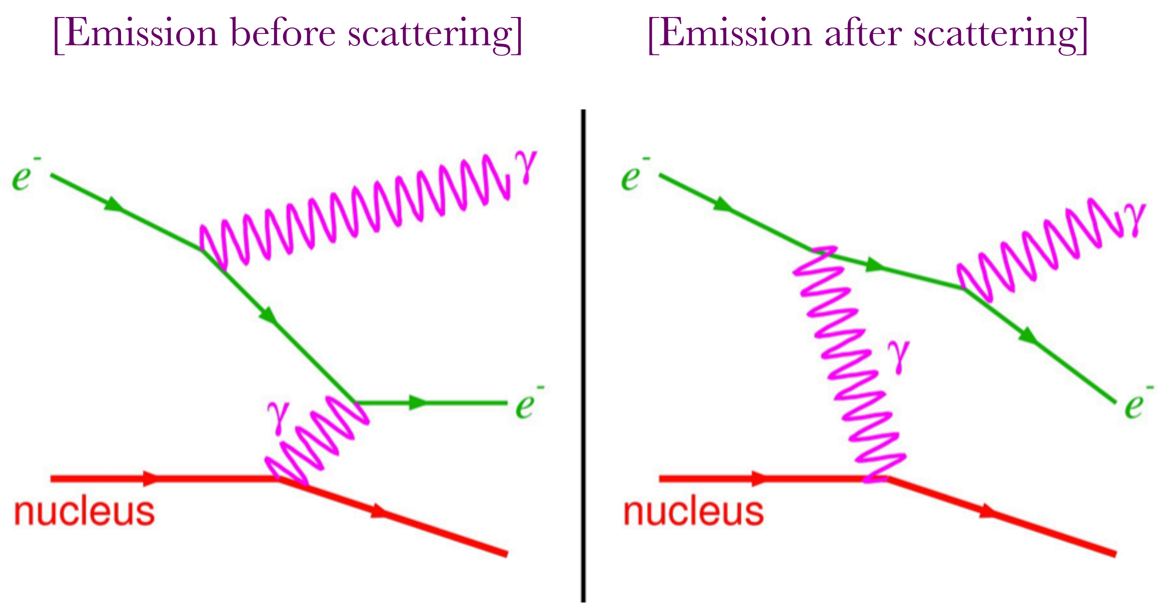

- *Left*: classical bremsstrahlung between an electron and a nucleus.
- *Right*: the quantum view – Feynman diagrams where the photon is emitted either <u>before</u> or <u>after</u> the Coulomb interaction.

2 Spectral Lines

We now draw these preliminary quantum concepts together to make a direct connection to solar and stellar spectroscopy. **C & O, Sec. 5.1**

The principal observation is that the solar spectrum is not a pure blackbody, but exhibits strong **absorption lines**.

Plot: Solar spectral lines

2.1 Kirchhoff's Laws

Kirchhoff summarized the production of spectral lines in stars via three succinct laws:

- *Hot dense* gas produces a continuous spectrum with no dark spectral lines;

- *Hot diffuse* gas produces bright spectral lines called **emission lines**;

- *Cool diffuse* gas in front of a source spectrum generates dark spectral lines (**absorption spectrum**).

Plot: Solar spectrum

Table: Strong solar lines

The goal is to now ascertain a physical basis for the nature of these laws, and characteristics of such lines. The basis is quantum mechanical in origin.

∗ The third of these laws establishes that stellar interiors are much hotter than their surfaces, an essential input for the theory of stellar structure.

Fraunhofer Lines in the Solar Spectrum

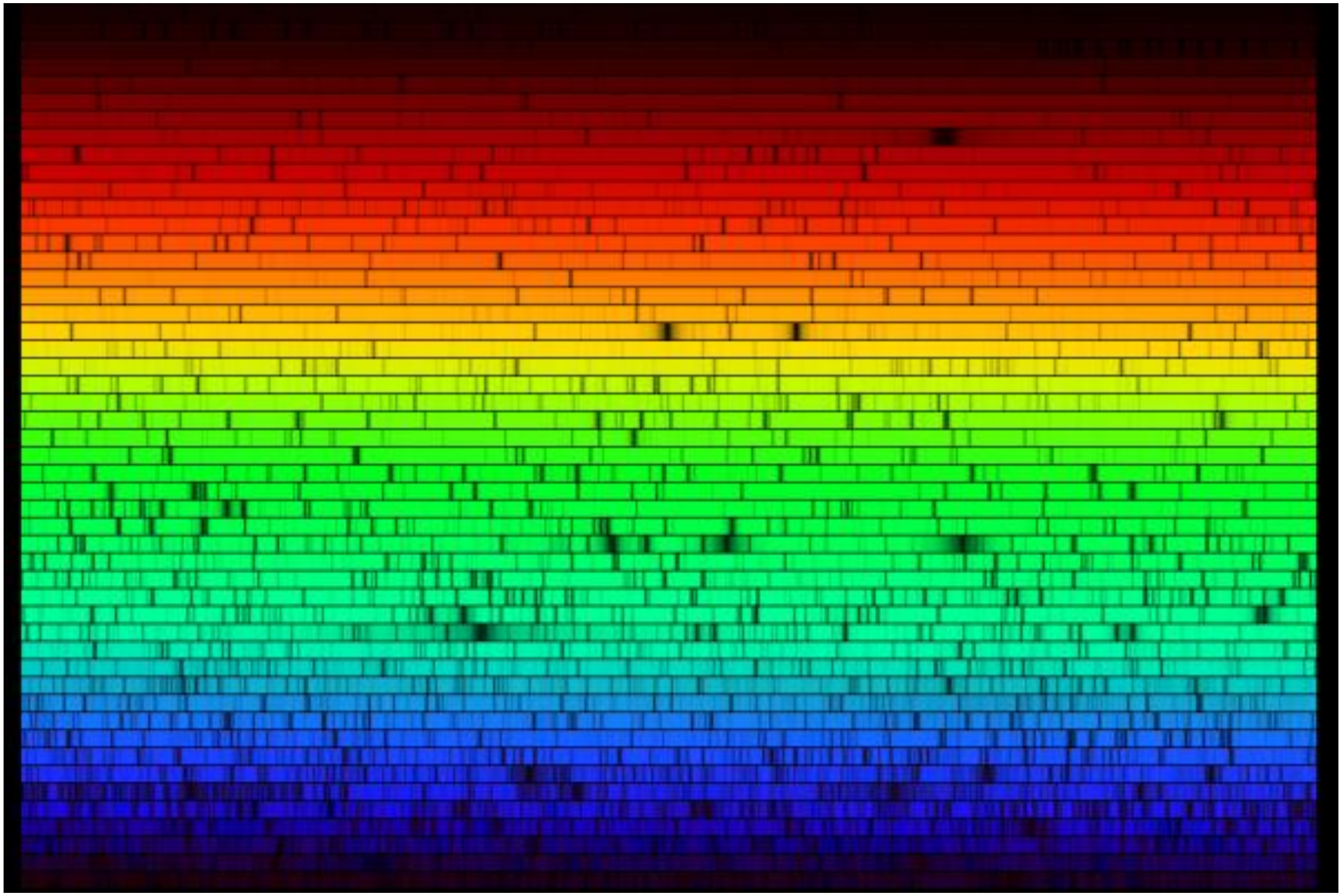

- Right: Rainbow representation of solar spectrum with absorption lines: [Courtesy NOAO]
- Left: 2012 German commemorative stamp celebrating Fraunhofer's 1787 birth.

The Solar Spectrum

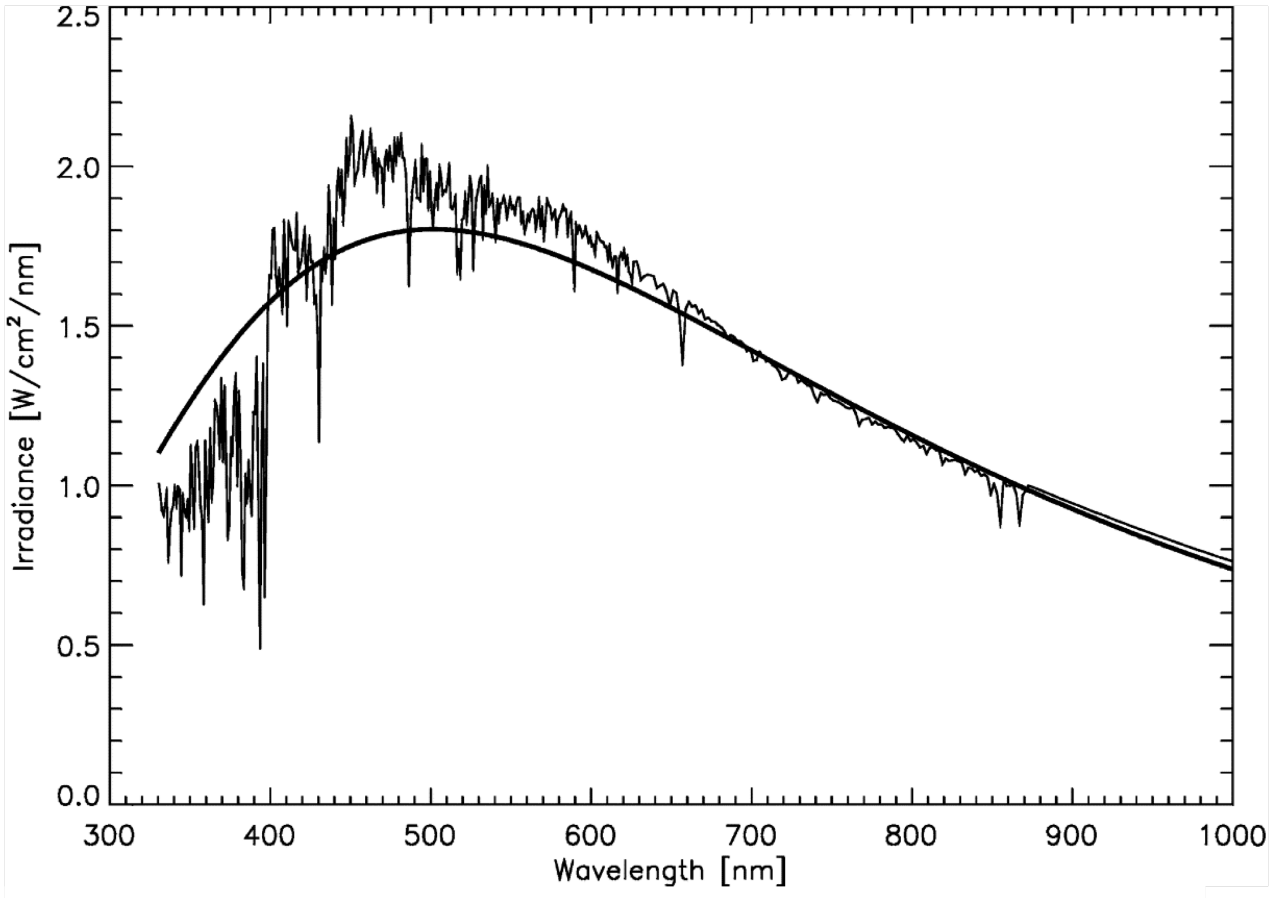

- The solar spectrum in visible and IR (300-1000nm) as measured by Neckel & Labs (1984, Sol. Phys. 90, 205). The fitted solid curve is a blackbody at 5770° K, the effective temperature of the photosphere.

Strong Fraunhofer Lines

Wavelength (Å)	Name	Atom	Equivalent Width (Å)
3859.922		Fe I	1.554
3886.294		Fe I	0.920
3905.532		Si I	0.816
3933.682	K	Ca II	20.253
3968.492	H	Ca II	15.467
4045.825		Fe I	1.174
4101.748	h, H_δ	H I	3.133
4226.740	g	Ca I	1.476
4340.475	G′, H_γ	H I	2.855
4383.557	d	Fe I	1.008
4404.761		Fe I	0.898
4861.342	F, H_β	H I	3.680
5167.327	b_4	Mg I	0.935
5172.698	b_2	Mg I	1.259
5183.619	b_1	Mg I	1.584
5889.973	D_2	Na I	0.752
5895.940	D_1	Na I	0.564
6562.808	C, H_α	H I	4.020

Table 5.1 Wavelengths of the Strong Fraunhofer Lines. The atomic notation is explained in Section 8.1, and the equivalent width of a spectral line is defined in Section 9.4. (Data from Lang, *Astrophysical Formulae*, Second Edition, Springer-Verlag, New York, 1980.)

Table 5.1 of Carroll & Ostlie, *Modern Astrophysics*.